



ELSEVIER

Journal of Computational and Applied Mathematics 147 (2002) 287–300

JOURNAL OF
COMPUTATIONAL AND
APPLIED MATHEMATICS

www.elsevier.com/locate/cam

Slip with friction and penetration with resistance boundary conditions for the Navier–Stokes equations—numerical tests and aspects of the implementation[☆]

Volker John*

*Institut für Analysis und Numerik, Otto-von-Guericke-Universität Magdeburg, Postfach 4120,
D-39016 Magdeburg, Germany*

Received 12 June 2001; received in revised form 2 January 2002

Abstract

We consider slip with friction and penetration with resistance boundary conditions in the steady state Navier–Stokes equations. This paper describes some aspects of the implementation of these boundary conditions for finite element discretizations. Numerical tests on two- and three-dimensional channel flows across a step using the slip with friction boundary condition study the influence of the friction parameter on the position of the reattachment point and the reattachment line of the recirculating vortex, respectively. © 2002 Elsevier Science B.V. All rights reserved.

Keywords: Navier–Stokes equations; Slip with friction boundary condition; Penetration with resistance boundary condition; Finite element methods

1. Introduction

The incompressible Navier–Stokes equations are a part of many complex models in science and applications. Often, other than the well understood no slip boundary condition of the velocity arise in these models. For instance, the Navier–Stokes equations in domains with free capillary boundaries require free slip boundary conditions, e.g., see [1]. Another example comes from the large eddy simulation (LES) of turbulent flows. The LES seeks to compute the large eddies of a turbulent flow accurately neglecting small flow structures. Galdi and Layton [4] propose to apply slip with friction and no penetration boundary conditions for the large eddies. Such boundary conditions are more

[☆] This work was partially supported by the DAAD (Deutsche Akademische Austauschdienst).

* Tel.: +49-391-67-12633; fax: +49-391-67-18073.

E-mail address: john@mathematik.uni-magdeburg.de (V. John).

suitable than Dirichlet boundary conditions to describe phenomena which can be observed in nature. E.g., the main vortices of a hurricane do not stick at the boundary such that homogeneous Dirichlet boundary conditions are not satisfied. These vortices move on the boundary (slip), losing energy while moving (friction) and do not penetrate the boundary. The last application, we like to mention, arises if a part of the boundary of the flow domain consists of porous material. Then, one has to take into account that the fluid may penetrate through the boundary. Altogether, one can observe a growing importance of slip with friction and penetration with resistance boundary conditions in applications.

Finite element methods are widely used discretizations of the incompressible Navier–Stokes equations. The use of these methods is of advantage especially in complex domains. Moreover, finite element methods allow the analysis of the arising discretizations. For no slip boundary conditions, we refer to [5] and the references therein. The mathematical properties of finite element discretizations of the Navier–Stokes equations with free slip boundary conditions are studied, e.g., in [14] and more recently in [10].

This paper describes some aspects of the implementation of the slip with linear friction and penetration with resistance boundary condition into a finite element discretization of the Navier–Stokes equations. The Navier–Stokes equations are linearized by a fixed point iteration. This boundary condition is implemented in such a way that it gives contributions to the matrix of the discrete system and the new iterate fulfils it in each step of the fixed point iteration. Numerical tests with the slip with friction boundary condition on the flow across a step in two and three dimensions study the dependency of the reattachment point and reattachment line, respectively, of the recirculating vortex on the friction parameter.

2. The Navier–Stokes equations and their finite element discretization

Let $\Omega \subset \mathbb{R}^d$, $d = 2, 3$, be a bounded domain with boundary $\partial\Omega = \Gamma_{\text{diri}} \cup \Gamma_{\text{sfpr}} \cup \Gamma_{\text{out}}$ such that all three parts of the boundary are mutually disjoint. The outer normal vector on $\partial\Omega$, which is assumed to exist almost everywhere on $\partial\Omega$, is denoted by $\mathbf{n}_{\partial\Omega}$. In addition, we use matrix vector notations, i.e., a vector \mathbf{v} is always a column vector and the corresponding row vector is denoted by \mathbf{v}^T . We consider the steady state incompressible Navier–Stokes equations in Ω

$$\begin{aligned} -\nu \Delta \mathbf{u} + (\mathbf{u} \cdot \nabla) \mathbf{u} + \nabla p &= \mathbf{f} \quad \text{in } \Omega, \\ \nabla \cdot \mathbf{u} &= 0 \quad \text{in } \Omega, \\ \mathbf{u} &= \mathbf{g} \quad \text{on } \Gamma_{\text{diri}}, \\ (2\nu \mathbb{D}(\mathbf{u}) - pI) \mathbf{n}_{\partial\Omega} &= \mathbf{0} \quad \text{on } \Gamma_{\text{out}}, \\ \mathbf{u} \cdot \mathbf{n}_{\partial\Omega} + \alpha \mathbf{n}_{\partial\Omega}^T (2\nu \mathbb{D}(\mathbf{u}) - pI) \mathbf{n}_{\partial\Omega} &= 0 \quad \text{on } \Gamma_{\text{sfpr}}, \\ \mathbf{u} \cdot \boldsymbol{\tau}_k + \beta^{-1} \mathbf{n}_{\partial\Omega}^T (2\nu \mathbb{D}(\mathbf{u}) - pI) \boldsymbol{\tau}_k &= 0 \quad \text{on } \Gamma_{\text{sfpr}}, \quad 1 \leq k \leq d-1. \end{aligned} \quad (1)$$

The unknown quantities are the velocity \mathbf{u} and the pressure p . The kinematic viscosity ν , the body force \mathbf{f} and the Dirichlet boundary conditions \mathbf{g} on Γ_{diri} are prescribed. Slip with linear friction and penetration with resistance boundary conditions are applied on Γ_{sfpr} . The penetration parameter α and the friction parameter β are given positive functions on Γ_{sfpr} . The unit tensor is denoted by I

and $\mathbb{D}(\mathbf{u})$ is the velocity deformation tensor

$$\mathbb{D}(\mathbf{u}) = \frac{\nabla \mathbf{u} + \nabla \mathbf{u}^T}{2}.$$

The tangential vectors τ_k , $1 \leq k \leq d - 1$ are chosen such that $\{\mathbf{n}_{\partial\Omega}, \tau_1\}$ in two dimensions and $\{\mathbf{n}_{\partial\Omega}, \tau_1, \tau_2\}$ in three dimensions build an orthonormal system of vectors. On Γ_{out} , an outflow or do-nothing boundary condition is prescribed.

We describe now the derivation of the discrete equations obtained by a finite element discretization. Let

$$\begin{aligned} V_{\mathbf{g}} &:= \{\mathbf{v} \in (H^1(\Omega))^d : \mathbf{v}|_{\Gamma_{\text{diri}}} = \mathbf{g}\}, \\ V_0 &:= \{\mathbf{v} \in (H^1(\Omega))^d : \mathbf{v}|_{\Gamma_{\text{diri}}} = \mathbf{0}\}, \\ Q &:= L^2(\Omega). \end{aligned}$$

The inner product in $(L^2(\Omega))^d$, $d = 1, 2, 3$, is denoted by (\cdot, \cdot) . The variational formulation of (1) is obtained in the usual way by multiplying (1) with a pair of test functions $(\mathbf{v}, q) \in (V_0, Q)$ and integrating the momentum equation by parts. The boundary condition on Γ_{sfpr} requires to use the deformation tensor formulation of the viscous term. Since $\nabla \cdot \mathbf{u} = 0$, it follows $\Delta \mathbf{u} = 2\nabla \cdot \mathbb{D}(\mathbf{u})$. The symmetry of the deformation tensor yields

$$\begin{aligned} (\mathbb{D}(\mathbf{u}), \nabla \mathbf{v}) &= \left(\mathbb{D}(\mathbf{u}), \frac{\nabla \mathbf{v}}{2} \right) + \left(\mathbb{D}(\mathbf{u})^T, \frac{\nabla \mathbf{v}^T}{2} \right) \\ &= \left(\mathbb{D}(\mathbf{u}), \frac{\nabla \mathbf{v}}{2} \right) + \left(\mathbb{D}(\mathbf{u}), \frac{\nabla \mathbf{v}^T}{2} \right) = (\mathbb{D}(\mathbf{u}), \mathbb{D}(\mathbf{v})). \end{aligned}$$

Thus, the weak problem is to find $(\mathbf{u}, p) \in (V_{\mathbf{g}}, Q)$ such that for all $(\mathbf{v}, q) \in (V_0, Q)$

$$\begin{aligned} 2\nu(\mathbb{D}(\mathbf{u}), \mathbb{D}(\mathbf{v})) + ((\mathbf{u} \cdot \nabla) \mathbf{u}, \mathbf{v}) - (p, \nabla \cdot \mathbf{v}) - \int_{\Gamma_{\text{sfpr}}} (2\nu \mathbb{D}(\mathbf{u}) - pI) \mathbf{n}_{\partial\Omega} \cdot \mathbf{v} \, ds &= (\mathbf{f}, \mathbf{v}), \\ (\nabla \cdot \mathbf{u}, q) &= 0. \end{aligned} \tag{2}$$

The boundary integral in the variational problem (2) can be rewritten by decomposing the test function \mathbf{v} on Γ_{sfpr} into d orthonormal components

$$\mathbf{v} = (\mathbf{v} \cdot \mathbf{n}_{\partial\Omega}) \mathbf{n}_{\partial\Omega} + \sum_{k=1}^{d-1} (\mathbf{v} \cdot \tau_k) \tau_k.$$

This gives, using the definition of the slip with linear friction and penetration with resistance boundary condition

$$\begin{aligned} &\int_{\Gamma_{\text{sfpr}}} (2\nu \mathbb{D}(\mathbf{u}) - pI) \mathbf{n}_{\partial\Omega} \cdot \mathbf{v} \, ds \\ &= \int_{\Gamma_{\text{sfpr}}} \mathbf{n}_{\partial\Omega}^T (2\nu \mathbb{D}(\mathbf{u}) - pI) \mathbf{n}_{\partial\Omega} \mathbf{v} \cdot \mathbf{n}_{\partial\Omega} \, ds + \int_{\Gamma_{\text{sfpr}}} \sum_{k=1}^{d-1} \mathbf{n}_{\partial\Omega}^T (2\nu \mathbb{D}(\mathbf{u}) - pI) \tau_k \mathbf{v} \cdot \tau_k \, ds \\ &= - \int_{\Gamma_{\text{sfpr}}} \alpha^{-1} (\mathbf{u} \cdot \mathbf{n}_{\partial\Omega}) (\mathbf{v} \cdot \mathbf{n}_{\partial\Omega}) \, ds - \int_{\Gamma_{\text{sfpr}}} \sum_{k=1}^{d-1} \beta (\mathbf{u} \cdot \tau_k) (\mathbf{v} \cdot \tau_k) \, ds. \end{aligned} \tag{3}$$

Thus, the variational problem can be reformulated: find $(\mathbf{u}, p) \in (V_{\mathbf{g}}, Q)$ such that for all $(\mathbf{v}, q) \in (V_0, Q)$

$$\begin{aligned}
 & 2v(\mathbb{D}(\mathbf{u}), \mathbb{D}(\mathbf{v})) + ((\mathbf{u} \cdot \nabla)\mathbf{u}, \mathbf{v}) - (p, \nabla \cdot \mathbf{v}) \\
 & + \int_{\Gamma_{\text{sfr}}} \alpha^{-1}(\mathbf{u} \cdot \mathbf{n}_{\partial\Omega})(\mathbf{v} \cdot \mathbf{n}_{\partial\Omega}) \, ds + \int_{\Gamma_{\text{sfr}}} \sum_{k=1}^{d-1} \beta(\mathbf{u} \cdot \boldsymbol{\tau}_k)(\mathbf{v} \cdot \boldsymbol{\tau}_k) \, ds = (\mathbf{f}, \mathbf{v}), \\
 & (\nabla \cdot \mathbf{u}, q) = 0.
 \end{aligned} \tag{4}$$

Remark 2.1. The boundary integrals which originate from the slip with friction and penetration with resistance boundary condition give a positive semi-definite contribution to the left-hand side of (4). The positivity follows from the positivity of α and β . Since the boundary integrals become zero for functions which vanish on Γ_{sfr} , they define a semi-definite operator. \square

Remark 2.2. In the computations presented in this report, the functions α and β are chosen to be piecewise constants on Γ_{sfr} . With the limits of these constants, other boundary conditions than slip with linear friction and penetration with resistance can be simulated. The choice $\alpha \rightarrow 0$ gives no penetration conditions. Choosing $\alpha \rightarrow \infty$ prescribes free penetration conditions. If $\alpha \rightarrow 0$, then the parameter $\beta \rightarrow 0$ prescribes free slip conditions on Γ_{sfr} whereas $\beta \rightarrow \infty$ sets no slip conditions (homogeneous Dirichlet boundary conditions).

The value of the friction coefficient β in model situations, applying wall laws for the velocity, was studied in [13]. \square

Eq. (4) is solved by a fixed point iteration starting with the initial iterate (\mathbf{u}^0, p^0) . Given (\mathbf{u}^m, p^m) , the iterate $(\mathbf{u}^{m+1}, p^{m+1})$ is computed by solving the variational problem for all $(\mathbf{v}, q) \in (V_0, Q)$

$$\begin{aligned}
 & 2v(\mathbb{D}(\mathbf{u}^{m+1}), \mathbb{D}(\mathbf{v})) + ((\mathbf{u}^m \cdot \nabla)\mathbf{u}^{m+1}, \mathbf{v}) - (p^{m+1}, \nabla \cdot \mathbf{v}) \\
 & + \int_{\Gamma_{\text{sfr}}} \alpha^{-1}(\mathbf{u}^{m+1} \cdot \mathbf{n}_{\partial\Omega})(\mathbf{v} \cdot \mathbf{n}_{\partial\Omega}) \, ds + \int_{\Gamma_{\text{sfr}}} \sum_{k=1}^{d-1} \beta(\mathbf{u}^{m+1} \cdot \boldsymbol{\tau}_k)(\mathbf{v} \cdot \boldsymbol{\tau}_k) \, ds = (\mathbf{f}, \mathbf{v}), \\
 & (\nabla \cdot \mathbf{u}^{m+1}, q) = 0, \quad m = 0, 1, 2, \dots .
 \end{aligned} \tag{5}$$

System (5) is a linear saddle point problem called Oseen equation. The Oseen equation is discretized by a finite element method. Let $(V_{\mathbf{g}}^h, Q^h)$ be a pair of finite element spaces and V_0^h the finite element test space for the velocity. The subscripts refer again to the Dirichlet boundary condition \mathbf{g} of the functions belonging to $V_{\mathbf{g}}$ and the homogeneous Dirichlet boundary conditions of the test functions. The discrete problem is to find $(\mathbf{u}^h, p^h) \in (V_{\mathbf{g}}^h, Q^h)$ such that for all $(\mathbf{v}^h, q^h) \in (V_0^h, Q^h)$

$$\begin{aligned}
 & 2v(\mathbb{D}(\mathbf{u}^h), \mathbb{D}(\mathbf{v}^h)) + ((\mathbf{u}_{\text{old}}^h \cdot \nabla)\mathbf{u}^h, \mathbf{v}^h) - (p^h, \nabla \cdot \mathbf{v}^h) + \int_{\Gamma_{\text{sfr}}} \alpha^{-1}(\mathbf{u}^h \cdot \mathbf{n}_{\partial\Omega})(\mathbf{v}^h \cdot \mathbf{n}_{\partial\Omega}) \, ds \\
 & + \int_{\Gamma_{\text{sfr}}} \sum_{k=1}^{d-1} \beta(\mathbf{u}^h \cdot \boldsymbol{\tau}_k)(\mathbf{v}^h \cdot \boldsymbol{\tau}_k) \, ds = (\mathbf{f}, \mathbf{v}^h), \\
 & (\nabla \cdot \mathbf{u}^h, q^h) = 0.
 \end{aligned} \tag{6}$$

The convection $\mathbf{u}_{\text{old}}^h$ is the current iterate of the velocity.

The matrix–vector form of (6) is

$$\begin{pmatrix} A(\mathbf{u}_{\text{old}}^h) & B \\ C & 0 \end{pmatrix} \begin{pmatrix} u \\ p \end{pmatrix} = \begin{pmatrix} f \\ 0 \end{pmatrix} \tag{7}$$

with

$$A(\mathbf{u}_{\text{old}}^h) = \begin{pmatrix} A_{11}(\mathbf{u}_{\text{old}}^h) & A_{12} \\ A_{21} & A_{22}(\mathbf{u}_{\text{old}}^h) \end{pmatrix} \quad \text{if } d = 2,$$

$$A(\mathbf{u}_{\text{old}}^h) = \begin{pmatrix} A_{11}(\mathbf{u}_{\text{old}}^h) & A_{12} & A_{13} \\ A_{21} & A_{22}(\mathbf{u}_{\text{old}}^h) & A_{23} \\ A_{31} & A_{32} & A_{33}(\mathbf{u}_{\text{old}}^h) \end{pmatrix} \quad \text{if } d = 3. \tag{8}$$

If $\Gamma_{\text{sfr}} = \emptyset$, the matrix blocks A_{ij} are determined by the viscous and the convective term. Since we have to use the deformation tensor formulation of the viscous term, none of the blocks A_{ij} vanishes and all blocks are in general mutually different. In the case $\text{meas}(\Gamma_{\text{sfr}}) > 0$, the implementation of the slip with friction and penetration with resistance boundary conditions, which will be described in the next section, gives in general contributions to each matrix block A_{ij} .

3. Aspects of the implementation of the slip with friction and penetration with resistance boundary conditions

In this section, some aspects of the implementation of the boundary integral term in (6)

$$\int_{\Gamma_{\text{sfr}}} \alpha^{-1}(\mathbf{u}^h \cdot \mathbf{n}_{\partial\Omega})(\mathbf{v}^h \cdot \mathbf{n}_{\partial\Omega}) \, ds + \sum_{k=1}^{d-1} \int_{\Gamma_{\text{sfr}}} \beta(\mathbf{u}^h \cdot \boldsymbol{\tau}_k)(\mathbf{v}^h \cdot \boldsymbol{\tau}_k) \, ds \tag{9}$$

coming from the slip with friction and penetration with resistance boundary conditions are described.

We describe the implementation for $d = 3$. The modifications in the two-dimensional case are obvious. Let $\{\mathbf{v}_j^a\}_{j=1}^{3N_v}$ be a basis of the velocity ansatz space $V_{\mathbf{g}}^h$ and $\mathbf{v}_i^t \in V_0^h$ be a test function which does not vanish on Γ_{sfr} . Typically, the basis and test functions of the velocity are chosen and ordered such that the first N_v functions do not vanish only in the first component, the second N_v functions in the second component and the last N_v functions in the third component, i.e.,

$$\mathbf{v}_j^a = \begin{pmatrix} v_{j1}^a \\ 0 \\ 0 \end{pmatrix} \quad \text{if } j \leq N_v, \quad \mathbf{v}_j^a = \begin{pmatrix} 0 \\ v_{j2}^a \\ 0 \end{pmatrix} \quad \text{if } N_v < j \leq 2N_v,$$

$$\mathbf{v}_j^a = \begin{pmatrix} 0 \\ 0 \\ v_{j3}^a \end{pmatrix} \quad \text{if } 2N_v < j \leq 3N_v.$$

With the following ansatz and notations:

$$\mathbf{u}^h = \sum_{j=1}^{3N_v} u_j \mathbf{v}_j^a, \quad \mathbf{v}_j^a = \begin{pmatrix} v_{j1}^a \\ v_{j2}^a \\ v_{j3}^a \end{pmatrix}, \quad \mathbf{v}_i^t = \begin{pmatrix} v_{i1}^t \\ v_{i2}^t \\ v_{i3}^t \end{pmatrix}, \quad \mathbf{n}_{\partial\Omega} = \begin{pmatrix} n_1 \\ n_2 \\ n_3 \end{pmatrix},$$

we obtain

$$\begin{aligned} & \int_{\Gamma_{\text{sfr}}} \alpha^{-1} (\mathbf{u}^h \cdot \mathbf{n}_{\partial\Omega}) (\mathbf{v}_i^t \cdot \mathbf{n}_{\partial\Omega}) \, ds \\ &= \sum_{j=1}^{3N_v} \alpha^{-1} u_j \int_{\Gamma_{\text{sfr}}} (v_{j1}^a n_1 + v_{j2}^a n_2 + v_{j3}^a n_3) (v_{i1}^t n_1 + v_{i2}^t n_2 + v_{i3}^t n_3) \, ds. \end{aligned}$$

This gives for $i \leq N_v$, i.e., for $v_{i2}^t = v_{i3}^t = 0$

$$\begin{aligned} & \int_{\Gamma_{\text{sfr}}} \alpha^{-1} (\mathbf{u}^h \cdot \mathbf{n}_{\partial\Omega}) (\mathbf{v}_i^t \cdot \mathbf{n}_{\partial\Omega}) \, ds \\ &= \sum_{j=1}^{3N_v} \alpha^{-1} u_j \left(\int_{\Gamma_{\text{sfr}}} v_{j1}^a v_{i1}^t n_1^2 \, ds + \int_{\Gamma_{\text{sfr}}} v_{j2}^a v_{i1}^t n_1 n_2 \, ds + \int_{\Gamma_{\text{sfr}}} v_{j3}^a v_{i1}^t n_1 n_3 \, ds \right). \end{aligned}$$

Similar formulas are obtained for $N_v < i \leq 2N_v$ and $2N_v < i \leq 3N_v$. If the integral

$$\alpha^{-1} \int_{\Gamma_{\text{sfr}}} v_{jl}^a v_{ik}^t n_l n_k \, ds, \quad k, l = 1, 2, 3,$$

does not vanish, it gives a contribution to the matrix entry $A_{kl}(i, j)$ of system matrix (8).

The other two terms of (9) are treated in a similar way. Let

$$\tau_1 = \begin{pmatrix} \tau_{11} \\ \tau_{12} \\ \tau_{13} \end{pmatrix}, \quad \tau_2 = \begin{pmatrix} \tau_{21} \\ \tau_{22} \\ \tau_{23} \end{pmatrix},$$

then the contribution to the matrix entry $A_{kl}(i, j)$ from (9) has the form

$$\alpha^{-1} \int_{\Gamma_{\text{sfr}}} v_{jl}^a v_{ik}^t n_l n_k \, ds + \beta \int_{\Gamma_{\text{sfr}}} v_{jl}^a v_{ik}^t (\tau_{1l} \tau_{1k} + \tau_{2l} \tau_{2k}) \, ds. \tag{10}$$

Remark 3.1. For $d = 2$, a tangential vector is immediately given by $\tau_1 = (n_2, -n_1)^T$. The only alternative tangential vector is $-\tau_1$ and it is obvious that the value of (10) does not depend on the choice of the tangential vector.

For $d = 3$, let τ_1, τ_2 be two arbitrary vectors which span the tangential plane such that $\{\mathbf{n}_{\partial\Omega}, \tau_1, \tau_2\}$ is a system of orthonormal vectors. One alternative choice of the system of tangential vectors is to reflect one of them, giving, e.g., the system $\{\mathbf{n}_{\partial\Omega}, \tau_1, -\tau_2\}$. Clearly, this alternative choice leaves (10) unchanged. Another way of changing the original systems of tangential vectors is to rotate them in the tangential plane around the axis $\mathbf{n}_{\partial\Omega}$ by the angle θ . This operation transforms the original system of orthonormal vectors into $\{\mathbf{n}_{\partial\Omega}, \tau_1 \cos \theta + \tau_2 \sin \theta, \tau_2 \cos \theta - \tau_1 \sin \theta\}$. It is a straightforward calculation to check that this operation also does not change (10). Altogether, also for $d = 3$

one can choose arbitrary tangential vectors τ_1, τ_2 such that $\{\mathbf{n}_{\partial\Omega}, \tau_1, \tau_2\}$ is a system of orthonormal vectors. \square

The tangential vectors are chosen in the computations presented in this report as follows.

Algorithm 3.2. *Computation of $\tau_1 = (\tau_{11}, \tau_{12}, \tau_{13})$ and $\tau_2 = (\tau_{21}, \tau_{22}, \tau_{23})$.* Given the normal vector $\mathbf{n}_{\partial\Omega} = (n_1, n_2, n_3)$ with the Euclidean norm $\|\mathbf{n}_{\partial\Omega}\|_2 = 1$. Then, there is at least one component n_i with $|n_i| \geq 0.5$.

```

1.  if ( $|n_1| \geq 0.5$  OR  $|n_2| \geq 0.5$ )
2.     $n := \sqrt{n_1^2 + n_2^2}$ 
3.     $\tau_{11} := n_2/n$ 
4.     $\tau_{12} := -n_1/n$ 
5.     $\tau_{13} := 0$ 
6.     $\tau_{21} := -\tau_{12}n_3$ 
7.     $\tau_{22} := \tau_{11}n_3$ 
8.     $\tau_{23} := \tau_{12}n_1 - \tau_{11}n_2$ 
9.  else
10.    $n := \sqrt{n_2^2 + n_3^2}$ 
11.    $\tau_{11} := 0$ 
12.    $\tau_{12} := -n_3/n$ 
13.    $\tau_{13} := n_2/n$ 
14.    $\tau_{21} := \tau_{13}n_2 - \tau_{12}n_3$ 
15.    $\tau_{22} := -\tau_{13}n_1$ 
16.    $\tau_{23} := \tau_{12}n_1$ 
17.  endif

```

The distinction of the two cases in Algorithm 3.2 ensures that a division by zero cannot happen.

Remark 3.3. The implementation of the slip with friction and penetration with resistance boundary condition for the time-dependent Navier–Stokes equations can be done in the analogous way as described in this section. A numerical example using this implementation, which computes a large eddy model of the time dependent Navier–Stokes equations, can be found in [7]. \square

Remark 3.4. An alternative approach to implement the slip with friction and penetration with resistance boundary condition is to use $\mathbf{u}_{\text{old}}^h$ instead of \mathbf{u}^h in the boundary integrals in (6). Then, the boundary integrals can be evaluated and they give contributions to the right-hand side of (7) instead to the system matrix. The evaluation of the boundary integrals requires also the evaluation of integrals of form (10). \square

4. Numerical studies

This section presents numerical tests for flows in a channel across a step in two and three dimensions. The most distinctive feature of these flows is a recirculating vortex behind the step,

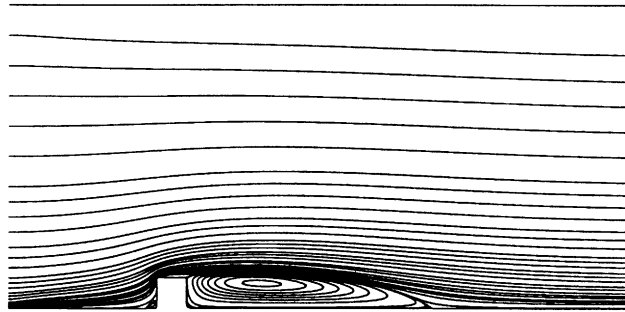


Fig. 1. Two-dimensional channel with a step, streamlines of the solution, $\nu^{-1} = 50$, parabolic inflow.

see Fig. 1 for an illustration. We will study the dependency of the position of the reattachment point in 2d and the reattachment line in 3d on the value of the friction parameter β .

We used in all computations the mapped Q_2/P_1^{disc} finite element. Given the reference mesh cell $\hat{K} = (-1, 1)^d$, we define

$$Q_2(\hat{K}) := \left\{ \sum_{i,j=0}^2 a_{ij} x_1^i x_2^j \right\}, \quad P_1(\hat{K}) := \left\{ \sum_{0 \leq i+j \leq 1} a_{ij} x_1^i x_2^j \right\} \quad \text{if } d = 2,$$

$$Q_2(\hat{K}) := \left\{ \sum_{i,j,l=0}^2 a_{ijl} x_1^i x_2^j x_3^l \right\}, \quad P_1(\hat{K}) := \left\{ \sum_{0 \leq i+j+l \leq 1} a_{ijl} x_1^i x_2^j x_3^l \right\} \quad \text{if } d = 3.$$

The spaces on an arbitrary mesh cell K are defined by the reference map $F_K: \bar{\hat{K}} \rightarrow \bar{K}$, where the overline denotes the closure,

$$Q_2(K) := \{ p = \hat{p} \circ F_K^{-1} : \hat{p} \in Q_2(\hat{K}) \}, \quad P_1(K) := \{ p = \hat{p} \circ F_K^{-1} : \hat{p} \in P_1(\hat{K}) \}$$

and the global spaces by

$$Q_2 := \{ v \in H^1(\Omega) : v|_K \in Q_2(K) \}, \quad P_1^{\text{disc}} := \{ v \in L^2(\Omega) : v|_K \in P_1(K) \}.$$

This conforming pair of finite element spaces fulfils the inf–sup or Babuška–Brezzi stability condition, see [11]. It is considered as a stable and well performing pair of elements for finite element discretizations of Navier–Stokes equations, e.g., see [2] or [6]. In addition, it has been proven to be superior to other pairs of finite elements in studies of benchmark problems for laminar flows [8,9].

The computations were performed only for such values of the viscosity parameter ν for which no additional stabilization for the reason of dominating convection was necessary. Thus, the influence of stabilization schemes on the computed results was avoided.

4.1. The two-dimensional flow across a step

The domain of the two-dimensional flow across a step is presented in Fig. 2. The same domain was used in computations in [3]. On the left-hand side, an inflow boundary condition is prescribed. We present results for a parabolic and a constant inflow profile. On the top and bottom boundary

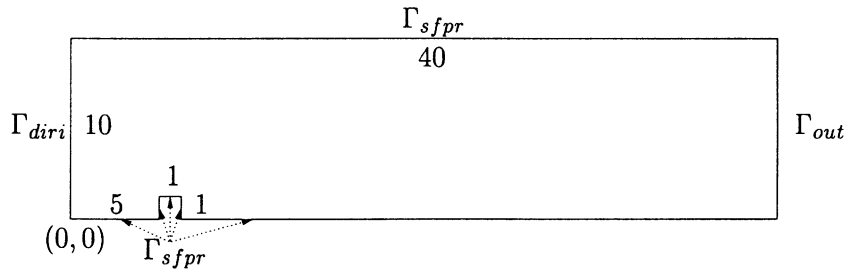


Fig. 2. Two-dimensional channel with a step.

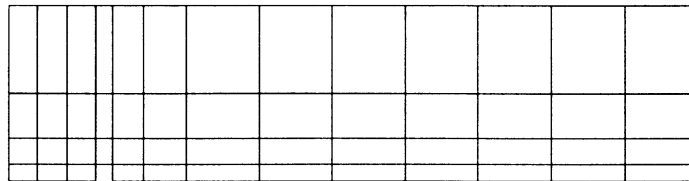


Fig. 3. Two-dimensional channel with a step, coarsest grid (level 0).

Table 1
Two-dimensional channel with a step, number of degrees of freedom

Level	Velocity	Pressure	Total
0	482	153	635
3	26690	9792	36482
4	105602	39168	144770
5	420098	156672	576770

as well as on the step, slip with friction and no penetration boundary conditions are prescribed. The no penetration property of the walls was imposed weakly by setting the parameter $\alpha = 10^{-12}$. The flow leaves the domain by an outflow boundary condition on the right-hand side of the channel.

We are interested in computing the reattachment point of the recirculating vortex behind the step. The end of the step is at the position $x = 6$. Since the tangential velocity on the bottom boundary does not vanish due to the slip with friction boundary condition, the reattachment point is defined by the change of the sign of the tangential velocity. Left of the reattachment point, the tangential velocity is negative because of the recirculation of the vortex and right of the reattachment point it is positive.

The computations were performed with the initial grid (level 0) presented in Fig. 3. The number of degrees of freedom for finer levels are given in Table 1. The fixed point iteration (5) was stopped if the Euclidean norm of the residual vector was $< 10^{-10}$.

Results for the parabolic inflow profile $\mathbf{u} = (u_1, u_2)^T$, with $u_1 = y(10 - y)/25$, $u_2 = 0$ on Γ_{dir} are presented for the viscosity parameters $\nu^{-1} = 50$ and $\nu^{-1} = 100$ in Figs. 4 and 5. For $\nu^{-1} = 100$, the

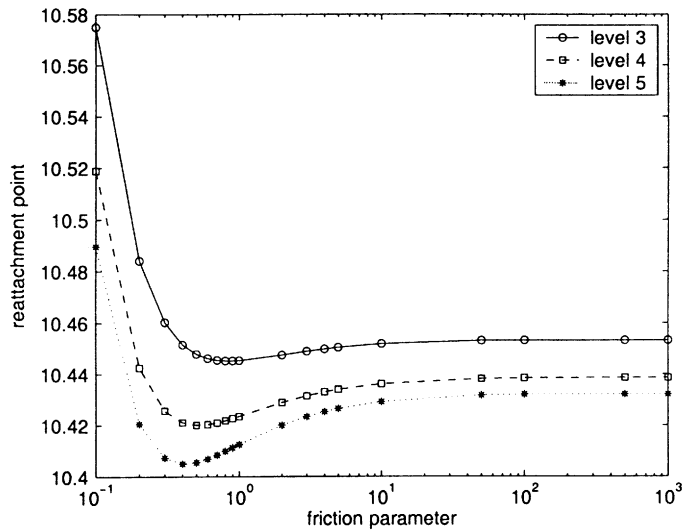


Fig. 4. Two-dimensional channel with a step, parabolic inflow profile, $\nu^{-1} = 50$.

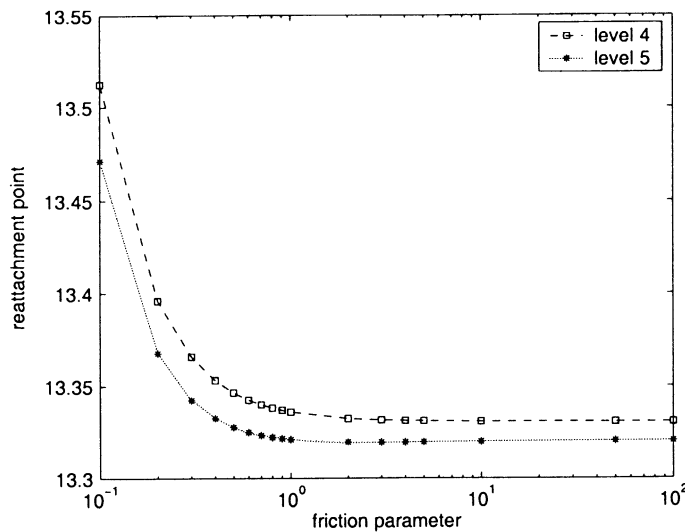


Fig. 5. Two-dimensional channel with a step, parabolic inflow profile, $\nu^{-1} = 100$.

position of the reattachment point moves towards the outflow boundary if the friction on the boundary decreases. For $\nu^{-1} = 50$, the reattachment point is naturally closer behind the step. There is a local minimum of the positions of the reattachment point. On level 5, this minimum is approximately at $\beta = 0.4$. But smaller values of the friction parameter leading again to a considerable movement of the reattachment point in the direction of the outflow boundary.

Figs. 6 and 7 present results which are computed for the constant inflow profile $u_1 = 1, u_2 = 0$ on Γ_{dir} . The results were obtained with the values $\nu^{-1} = 50$ and $\nu^{-1} = 100$ for the viscosity. The position

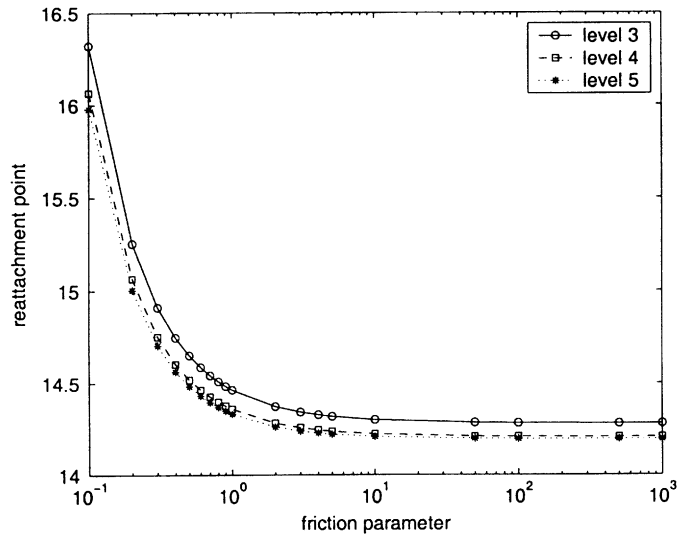


Fig. 6. Two-dimensional channel with a step, constant inflow profile, $v^{-1} = 50$.

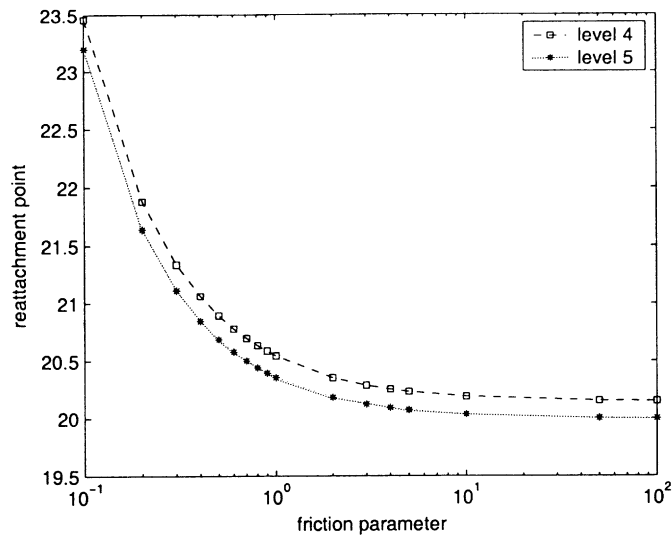


Fig. 7. Two-dimensional channel with a step, constant inflow profile, $v^{-1} = 100$.

of the reattachment point moves in all computations towards the outflow boundary for smaller values of the friction parameter β .

Remark 4.1. The position of the reattachment point for large values of β is very close to the position of this point using no slip boundary conditions on the bottom and top wall. It can be observed that

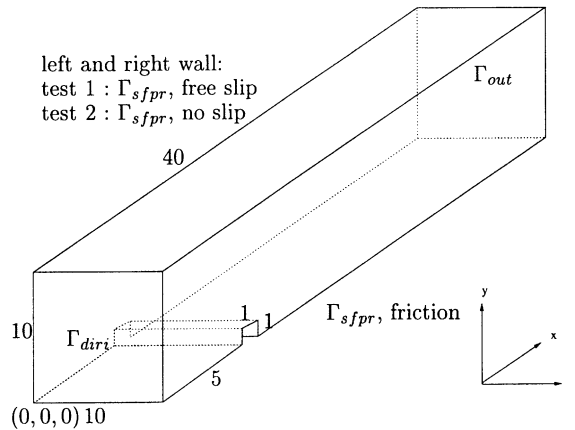


Fig. 8. Three-dimensional channel with a step.

Table 2
Three-dimensional channel with a step, number of degrees of freedom

Level	Velocity	Pressure	Total
0	7953	1020	8973
1	56007	8160	64167
2	419307	65280	484587

it is in general not possible to catch the reattachment point for no slip boundary conditions on a fine level by an appropriate choice of β on a coarse level. \square

Remark 4.2. One can think of applying no slip boundary conditions weakly by choosing a large value of the friction parameter β . However, in our computations, we could not solve the arising systems of equations for large values of β . We applied as solver the flexible GMRES method defined in [12] with a so-called multiple discretization multilevel method, as introduced in [8,9], as preconditioner. This solver has been proven to be very robust and efficient in a benchmark problem for the Navier–Stokes equations [9]. We think that the problems in the solution of the linear system are caused by the growing dominance of a semi-definite operator in the system matrix for large β , see Remark 2.1. Thus, no slip boundary conditions should be applied always in the standard way by setting the degrees of freedom on the boundary. \square

4.2. The three-dimensional flow across a step

The domain as well as the boundary conditions in these tests are given in Fig. 8. In the first test, we applied free slip boundary conditions at the left and right wall and in the second test no slip boundary conditions. At the inflow, the constant inflow profile $u_1 = 1, u_2 = u_3 = 0$ was prescribed. The no penetration condition was again imposed weakly by setting $\alpha = 10^{-12}$.

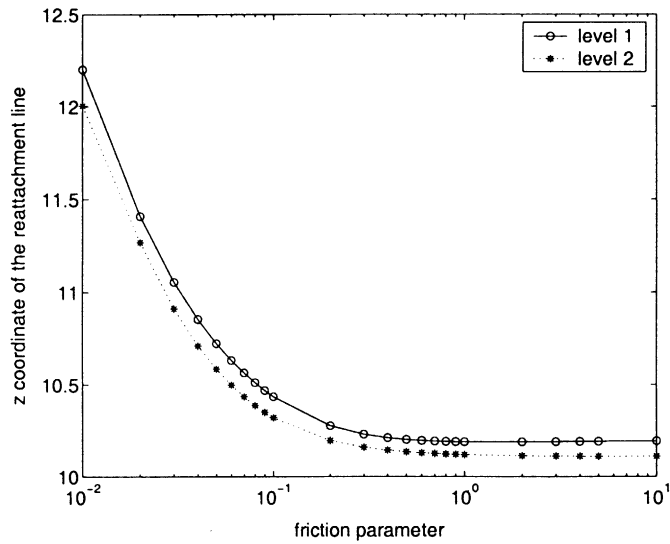


Fig. 9. Three-dimensional channel with a step, slip boundary conditions at the lateral boundaries, $\nu^{-1} = 20$.

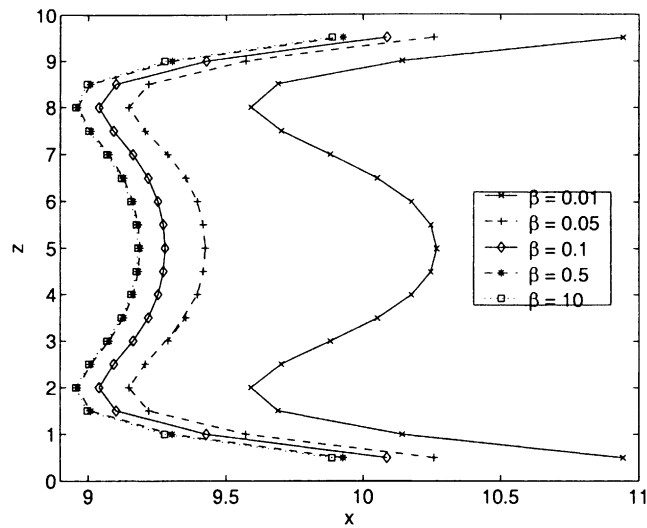


Fig. 10. Three-dimensional channel with a step, reattachment line for no slip boundary conditions at the lateral boundaries, $\nu^{-1} = 20$.

The initial grid is generated by the so-called sandwich grid technique. The grid presented in Fig. 3 can be seen on the left and the right wall of the domain and in between there are five equal sized layers of mesh cells. The corresponding numbers of degrees of freedom arising in the Q_2/P_1^{disc} finite element discretization are given in Table 2. The fixed point iteration (5) was stopped if the Euclidean norm of the residual was $< 10^{-10}$.

Using free slip conditions on the left and right wall gives a flow field which is independent of z . Thus, the reattachment point for each value of z is the same and the reattachment line is a straight line. We present the coordinate of this straight line for the viscosity parameter $\nu^{-1} = 20$ in Fig. 9. As in the two-dimensional tests, the reattachment line moves toward the outflow boundary if the friction parameter is chosen smaller.

Applying no slip boundary conditions at the left and the right wall, one gets reattachment lines which are symmetric for $z = 5$, see Fig. 10. The computations in this test were performed on level 2. As expected, the reattachment line is the closer to the outflow boundary the smaller the friction parameter β is. But there are only small differences in the position of this line for $\beta = 0.5$ and $\beta = 10$.

As in the two-dimensional computations, the use of larger values of β then presented here failed because we could not solve the arising systems of equations, see Remark 4.2.

References

- [1] E. Bänsch, Finite element discretization of the Navier–Stokes equations with free capillary surface, *Numer. Math.* 88 (2001) 203–235.
- [2] M. Fortin, Finite element solution of the Navier–Stokes equations, In: A. Iserles (Ed.), *Acta Numerica*. Cambridge University Press, 1993, pp. 239–284.
- [3] V.P. Fragos, S.P. Psychoudaki, N.A. Malamataris, Computer-aided analysis of flow past a surface-mounted obstacle, *Internat. J. Numer. Methods Fluids* 25 (1997) 495–512.
- [4] P. Galdi, W. Layton, Approximation of the larger eddies in fluid motion ii: a model for space filtered flow, *Math. Models Methods Appl. Sci.* 10 (3) (2000) 343–350.
- [5] V. Girault, P.-A. Raviart, *Finite Element Methods for Navier–Stokes Equations*, Springer, Berlin, Heidelberg, New York, 1986.
- [6] P.M. Gresho, R.L. Sani, *Incompressible Flow and the Finite Element Method*, Wiley, New York, 2000.
- [7] T. Iliescu, V. John, W.J. Layton, Convergence of finite element approximations of large eddy motion, *Numer. Methods Partial Differential Equations*, accepted for publication, 2002.
- [8] V. John, G. Matthies, Higher order finite element discretizations in a benchmark problem for incompressible flows, *Intern. J. Numer. Methods Fluids* 37 (2001) 885.
- [9] V. John, Higher order finite element methods and multigrid solvers in a benchmark problem for the 3D Navier–Stokes equations, *Intern. J. Numer. Methods Fluids*, accepted for publication, 2002.
- [10] A. Liakos, Discretization of the Navier–Stokes equations with slip boundary condition, *Numer. Methods Partial Differential Equation* 17 (2001) 26–42.
- [11] G. Matthies, L. Tobiska, The inf–sup condition for the mapped $Q_k - P_{k-1}^{\text{disc}}$ element in arbitrary space dimensions, *Computing*, accepted for publication, 2002.
- [12] Y. Saad, A flexible inner-outer preconditioned GMRES algorithm, *SIAM J. Sci. Comput.* 14 (2) (1993) 461–469.
- [13] V. John, W.J. Layton, N. Sahin, Derivation and analysis of near wall models for channel and recirculating flows. Preprint 14/02, Fakultät für Mathematik, Otto-von-Guericke-Universität Magdeburg, 2002.
- [14] R. Verfürth, Finite element approximation of incompressible Navier–Stokes equations with slip boundary condition, *Numer. Math.* 50 (1987) 697–721.